Electron-phonon coupling and d-wave superconductivity in the cuprates

Jinsuk Song* and James F. Annett†
Department of Physics, The Pennsylvania State University, University Park, Pennsylvania 16802
(Received 5 October 1994)

We derive an effective single-band Hubbard-type Hamiltonian for CuO_2 planes in the cuprate high-T_c superconductors. The Hamiltonian includes both electron-electron repulsion and electron-phonon coupling to oxygen vibrational modes. The effective Hamiltonian is derived by mapping from the multiband constrained-density-functional-theory Hamiltonian to a one-band model. A Hartree-Fock mapping leads to $t = 0.66$ eV, $t' = -0.14$ eV, and $U = 4.0$ eV. Very similar parameters are obtained by exact diagonalization of finite clusters. The electron-phonon coupling to oxygen breathing modes gives $\lambda = 0.57$ for s-wave and $\lambda = 0.35$ for $d_{x^2-y^2}$ pairing. d-wave superconductivity is predicted to occur at 30 K for doped La_2CuO_4, while the strong Coulomb repulsion suppresses the s-wave T_c to 10 K.

I. INTRODUCTION

Ever since the discovery of the cuprate high-temperature superconductors by Bednorz and Müller[1] there has been debate over whether the high T_c is due to a purely electronic mechanism for superconductivity or whether electron-phonon coupling plays a role in the pairing. It soon became apparent that a standard Eliashberg formulation of phonon-mediated pairing could not account for the high transition temperatures.[2] The small oxygen isotope effects in $YBa_2Cu_3O_7$ also suggested a purely electronic mechanism for the superconductivity.[3] This led to a considerable theoretical effort to derive purely electronic mechanisms for high-temperature superconductivity. More recently, this picture has been supported by a large body of experimental evidence showing that the superconducting state in $YBa_2Cu_3O_7$ is almost certainly a d-wave state with x^2-y^2 symmetry.[4–7] The d-wave superconductivity could be caused by the exchange of antiferromagnetic spin fluctuations without any contribution from phonons.[8] Numerical studies of the two-dimensional (2D) Hubbard model have also suggested that it may have a $d_{x^2-y^2}$ superconducting ground state purely due to repulsive electron-electron interactions.[9]

On the other hand, weak isotope effects and a probable d-wave pairing state do not prove conclusively that electron-phonon coupling is irrelevant. It is a clear experimental fact that electron-phonon coupling *is* present in the cuprates. For example, Raman and infrared studies show Fano line shapes for many of the phonons as well as significant frequency and linewidth changes at T_c.[10] These experiments imply that the phonons are indeed coupled to the charge carriers, and are significantly affected when the superconducting gap opens. A large isotope effect has also been observed in the $Ba_{1-x}K_xBiO_3$ superconductors,[11] and it appears probable that the Nd based "n-type" cuprate superconductors are s-wave superconductors[12] which can be understood in a conventional Eliashberg formalism.[13] Measurements also show a substantial oxygen isotope effect in $La_{2-x}Sr_xCuO_4$ and anomalously large copper isotope effects,[14] implying that the phonon coupling contributes at least partially to the T_c.

It seems unlikely that a purely electronic superconductivity mechanism operates in some of these materials while ordinary phonon-mediated pairing occurs in others. A more plausible scenario is that *both* electron-electron repulsion and electron-phonon coupling effects are present. Possibly in some materials the phonon coupling is dominant and s-wave pairing results, while in other systems the Coulomb repulsion is larger and antiferromagnetic spin fluctuations are stronger, driving up T_c in the d-wave channel. Indeed, a phonon-mediated attraction can contribute to the T_c even in a d-wave superconductor provided the electron-phonon interactions are spatially nonlocal. For example, two holes on adjacent copper sites may experience an attractive interaction due to motion of the intervening oxygen atom. By forming a d-wave Cooper pair they can bind in the nonlocal attractive potential without any penalty from the strong local on site repulsion U. We show below that this mechanism does indeed take place in the cuprates, and that d-wave superconductivity with a moderately high transition temperature is possible even without invoking enhancements due to antiferromagnetic spin fluctuations or interlayer coupling.

The purpose of this paper is to develop a realistic model Hamiltonian which includes *both* the electron-electron repulsion and the electron-phonon coupling in the cuprates. Both interactions are clearly present in the experimental systems and a complete theory must include them both, if only to show that one or the other is ultimately irrelevant. Our goal is to derive a Hamiltonian in which there are no free parameters, starting from first principles electronic structure calculations. Furthermore the Hamiltonian should include all of the relevant physics of the copper oxide planes. For example, the detailed shape of the Fermi surface should be included,

0163-1829/95/51(6)/3840(10)/$06.00

unlike, say, the simple nearest neighbor Hubbard model. Also, the couplings to all of the various oxygen vibration modes should be included, unlike a simple Hubbard-Holstein model. The model Hamiltonian should ideally also be simple to write down and to understand. For this reason a one-band model is to be preferred over the full multiband Hubbard models of the copper oxide planes, provided the one-band model includes all of the relevant low-energy physics.

Below, we base our calculation on the mapping from density-functional-theory (DFT) electronic-structure to *ab initio* Hubbard models.[15,16] This provides a framework in which both electron-electron repulsion and electron-phonon coupling can be naturally included. We show that the mapping from the full multiple-band Hubbard model of the cuprates to an effective low-energy single-band Hamiltonian leads to realistic electron-phonon coupling parameters. To estimate the robustness of this renormalization down to the low-energy effective Hamiltonian we carry out the mapping in two quite different ways, either using exact diagonalization of small clusters or a Hartree-Fock-based method. The former allows a complete description of the many-body correlations, and is a straightforward extension of the the earlier mappings from multiple-band to single-band Hubbard models by Hybertsen *et al.*[17] and Bacci *et al.*[18] The Hartree-Fock approach, on the other hand, treats the correlations approximately, but allows a more realistic treatment of the Fermi surface shape and the momentum dependence of the interactions.

In examining the oxygen vibrational modes we have concentrated on the planar oxygen atoms, including both in-plane and out-of-plane motion. The planar oxygens are the only ones present in *all* of the cuprate superconductors, and they interact most strongly with the charge carriers localized in the planes. Motion of the oxygen along the bond direction corresponds to the high-energy breathing modes and the strongest linear electron-phonon coupling terms.[2,19,20] On the other hand, motion of the planar oxygen perpendicular to the planes corresponds to the buckling and tilting of the CuO_2 plane. In $La_{2-x}R_xCuO_4$ the tilting mode leads to the lattice instability from the tetragonal to orthorhombic phase. These phonons are therefore quite anharmonic.[21] For $YBa_2Cu_3O_7$ a similar oxygen z motion leads to the static buckling of the CuO_2 plane. The anharmonicity of oxygen modes has motivated a number of theories of superconductivity derived from double-well potentials and dynamic Jahn-Teller effects[22,23] or other effects of strong lattice anharmonicity.[25–27] Neutron scattering[28] and analysis of other experiments[29] provides direct evidence for only a moderate degree of anharmonicity for these modes, even in $La_{2-x}R_xCuO_4$.

A. Constrained DFT Hamiltonian

In defining electron-phonon coupling matrix elements it is necessary to start with a model for the electronic structure. The most commonly used method is to develop a tight-binding fit to the density-functional-theory band structure. For example, Weber and Mattheiss[2] used this method in their original work on La_2CuO_4 and $YBa_2Cu_3O_7$. A more accurate method, used by Cohen *et al.*,[20] carries out a direct calculation of the matrix elements in the "deformation" in the single-particle potential caused by a phonon displacement. However, neither of these methods fully takes into account the strong electron-electron repulsions. For example, the true quasiparticle bands are strongly renormalized relative to the Kohn-Sham local-density-approximation (LDA) bands by the interactions. Furthermore, single-particle matrix elements computed with Kohn-Sham potentials and wave functions have no formal correspondence with the Landau Fermi-liquid quasiparticle-phonon matrix elements which are the starting point of BCS theory. As an alternative we determine the electron-phonon coupling from an explicit many-body picture of the electronic structure, derived from constrained density functional theory.[15]

The constrained DFT model for the electronic structure of the cuprates explicitly includes the effects of the electron-electron interactions, while remaining free of adjustable parameters.[15] A set of localized Wannier functions are derived from the ordinary DFT band structure. Hopping among these Wannier orbitals defines a tight-binding Hamiltonian. On-site Coulomb interactions are estimated by setting the hopping to zero on a given Wannier orbital, and computing the total energy as a function of the Wannier orbital occupation. The Hubbard U for that site is determined by the second derivative of the DFT energy with occupation. Although not completely rigorous, this method provides a parameter-free mapping from a realistic electronic structure to an extended Hubbard model. For the cuprates this multiple-band Hamiltonian is given by

$$\hat{H} = \hat{H}_d + \hat{H}_p + \hat{H}_{pd} \ , \tag{1}$$

where

$$\hat{H}_d = \epsilon_d \sum_{i,\sigma} d^\dagger_{i,\sigma} d_{i,\sigma} + U_d \sum_i n_{i\uparrow} n_{i\downarrow}, \tag{2}$$

$$\hat{H}_p = \epsilon_p \sum_{l,\sigma} p^\dagger_{l,\sigma} p_{l,\sigma} + U_p \sum_l n_{l\uparrow} n_{l\downarrow} + \sum_{\langle l,l'\rangle,\sigma} t^{ll'}_{pp} (p^\dagger_{l,\sigma} p_{l',\sigma} + \text{H.c.}) \tag{3}$$

$$\hat{H}_{pd} = \sum_{\langle i,l\rangle,\sigma} t^{il}_{pd} (d^\dagger_{i,\sigma} p_{l,\sigma} + \text{H.c.}) + U_{pd} \sum_{\langle il\rangle} n_i n_l. \tag{4}$$

The operator $d^\dagger_{i,\sigma}$ creates a Cu_{3d} hole at site i and $p^\dagger_{l,\sigma}$ creates an O_{2p} hole at site l. In most of our calculations we only include the $Cud_{x^2-y^2}$ orbitals and the two oxygen p_σ states per CuO_2 unit cell. However, for calculations with out-of-plane oxygen vibrational modes we also include the two planar oxygen p_z orbitals; i.e., we have a five-band Hamiltonian.

The parameters in this constrained DFT Hamiltonian have been derived directly from first principles calculations.[15,16] We used the parameter values for La_2CuO_4 derived by McMahan *et al.*[15] These values are very similar to those derived by Hybertsen *et al.*[16] using

a slightly different method. These parameters are also consistent with other independent estimates,[30] although a quite different picture has also been proposed.[31] The constrained DFT parameter values are also in agreement with a number of experimental features, including Cu d two-hole resonances in photoemission,[15] NMR chemical shifts,[32] and the antiferromagnetic exchange parameter J.[17,32] A similar "LDA+U" approach to DFT band structure plus Hubbard interactions is also thought to account for a wide range of phenomena in various transition metal and rare earth compounds.[33,34]

Electron-phonon coupling can be incorporated into this many-body Hamiltonian by considering static frozen phonon lattice distortions. In order to extract an electron-phonon coupling it is necessary to know the variations of the Hamiltonian parameters with phonon displacements. Repeating the full constrained DFT mapping as a function of phonon displacements has not been done, since it would be very time consuming. However, it is clear that the dominant oxygen mode contributions will come from the change in copper-oxygen hopping with Cu-O bond length or angle. An estimate of these changes can be obtained simply by expressing the pd hopping parameters in terms of Slater-Koster parameters $V_{pd\sigma}$ and $V_{pd\pi}$, and assuming that these vary with bond length like $r^{-7/2}$. This distance and angle dependence corresponds to the canonical tight-binding[35] description of the single-particle hopping Hamiltonian in Eq. (1). As such it is a reasonable leading-order estimate. In fact, this assumed distance dependence of $V_{pd\sigma}$ and $V_{pd\pi}$ is essentially identical to the one determined by Weber[2] using fits to the band structures at two different lattice constants. In our calculations we neglected any changes in t_{pp} with the oxygen displacements, since these will make only a small contribution.

II. MAPPING TO A SINGLE-BAND HAMILTONIAN

In practice the full multiple-band Hamiltonian is hard to solve and it is preferable to reduce the Hamiltonian to an effective single-band model. The single-band model contains the same low-energy physics, but is easier to solve numerically and to understand. For the cuprates the appropriate one-band model consists of a Hubbard-like Hamiltonian

$$\hat{H} = \hat{H}_e + \hat{H}_{e-e}. \tag{5}$$

The single-particle hopping part is

$$\hat{H}_e = t \sum_{\langle i,j\rangle,\sigma} (c^\dagger_{i,\sigma} c_{j,\sigma} + \text{H.c.}) + t' \sum_{\langle\langle i,k\rangle\rangle,\sigma} (c^\dagger_{i,\sigma} c_{k,\sigma} + \text{H.c.}) , \tag{6}$$

where $c^\dagger_{i\sigma}$ creates a hole in a Wannier orbital centered on copper site i. Here $\langle i,j\rangle$ and $\langle\langle i,k\rangle\rangle$ indicate nearest neighbor and next nearest neighbor pairs, respectively. Since we are working in a hole representation appropriate for the p-type cuprates, the signs of t and t' are chosen corresponding to hole not electron dispersion. The hole-hole interaction is described by a generalized Hubbard form

$$\hat{H}_{e-e} = U \sum_i n_{i\uparrow} n_{i\downarrow} + U' \sum_{\langle i,j\rangle} n_i n_j + \cdots . \tag{7}$$

The parameters in this effective one-band model are defined by requiring that it contain the same low-energy physics as the full Hamiltonian. In essence this mapping from a multiple-band to single-band Hamiltonian is a renormalization procedure, in which high-energy states are "integrated out" to leave a new low-energy model.[17] This renormalization can be carried out in a variety of different ways, and we have used two complimentary methods in this work.

The first method used to map from the multiple-band model to a one-band Hamiltonian uses exact many-body diagonalization. The full many-body eigenstates of the Hamiltonian (1) can be found exactly in small clusters by the Lanczos method. These eigenvalues are then compared to the corresponding eigenvalues for the simpler one-band Hubbard or $t-J$ model. Provided a reasonable correspondence among the many-band and single-band eigenvalues exists it is straightforward to vary the single-band parameters to obtain the best fit. Conversely, if a good fit cannot be obtained, we can conclude that the low energy states of the multiple-band model cannot be mapped to the simpler one-band model; i.e., the higher bands are "relevant" for the low-energy physics. This procedure was carried out previously by Hybertsen *et al.*[17] and by Bacci *et al.*[18] For the cuprate Hamiltonian given in Eq. (1) Hybertsen *et al.*[17] concluded that a good fit could be obtained using the $t-t'-J$ model with $t = 0.41$ eV, $t' = -0.07$ eV, and $J = 0.128$ eV or the Hubbard model with $U = 5.4$ eV and the same values of t and t'. Bacci *et al.*[18] found a best fit corresponding to about $t = 0.54$ eV and $U = 3.0$ eV (assuming $t' = 0$), with t and U varying only slightly with changes in the multiple-band Hamiltonian parameter values.

As a starting point for our electron-phonon coupling calculations we first repeated the calculation of Bacci *et al.*[18] Figure 1 shows the lowest six eigenvalues of a Cu_4O_8 cluster with four holes, and the mapping to the corresponding eigenstates of the 2×2 Hubbard model.

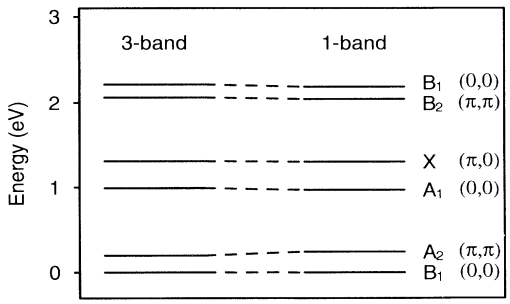

FIG. 1. The mapping of the lowest energy levels of a Cu_4O_8 cluster with four holes between the multiple-band and single-band Hubbard Hamiltonians. The best-fit single-band parameters are $t = 0.48$ eV, $U = 3.2$ eV.

The correspondence of levels of the three- and one-band models is excellent, as shown in Fig. 1, implying that the low-energy physics of the three-band model does indeed correspond to the single-band Hubbard model. The best fit to the spectrum was found for the one-band parameters $t = 0.48$ eV and $U = 3.2$ eV. These parameters are very close to the values found previously by Bacci *et al.*,[18] and the slight differences arise from our full inclusion of U_p and U_{pd} in the multiple-band Hamiltonian. Note that it is not possible to reliably extract a second neighbor hopping t' for such a small cluster, since each site has only one second neighbor. In principle t' could be found in calculations for larger clusters. Unfortunately the Lanczos method is limited to very small cluster sizes because of the exponential growth in the Hilbert space with cluster size. The next large size cluster with periodic boundaries and a bipartite lattice is Cu_8O_{16} which has over 10^7 states at half filling.

We also found a second method to be useful in the renormalization from the multiple-band to a single-band model. This method starts with the Hartree-Fock solution of the multiple-band model. The advantage of this method is that it avoids the limitation to small clusters imposed by the exact diagonalization scheme. The Hartree-Fock solution allows calculations in the infinite lattice limit, although it treats the correlations approximately. In the Hartree-Fock solution it is straightforward to obtain the band structure and Fermi surface. Figure 2 shows the Fermi surface and energy band contours for the lowest band, at a hole doping of 0.125. The band structure and Fermi surface are very similar to the LDA energy bands and Fermi surface of La_2CuO_4.[36,37] Since there is only one band close to the Fermi energy, we can define an effective single-band model by fitting this band. Choosing parameters so that the one-band model exactly reproduces the shape of the Hartree-Fock Fermi surface and the Fermi surface band velocities leads to $t = 0.66$ eV and $t' = -0.14$ eV, where t' is the next nearest neighbor hopping. t' is essential in order to obtain the correct shape of the Fermi surface in Fig. 2, which is clearly quite different from the nearest-neighbor-only Hubbard model. This could be very significant since, unlike the nearest neighbor model, the Fermi energy lies very close to a Van Hove singularity corresponding to the flat bands at the M point (within 0.07 eV at this doping). Several authors have pointed out that the presence of a Van Hove singularity so close to the Fermi energy could be a significant factor in enhancing the superconducting T_c.[38,39]

Within the Hartree-Fock method we can also determine the electron-electron interactions, and map these into a one-band Hubbard model. First we compute the matrix elements of the Coulomb interaction between holes at the Fermi surface, using the multiple-band model:

$$V(\mathbf{k}_1,\mathbf{k}_2,\mathbf{k}_3,\mathbf{k}_4) = \langle \mathbf{k}_1,\mathbf{k}_2|\hat{H}_{e-e}|\mathbf{k}_3,\mathbf{k}_4\rangle \ , \qquad (8)$$

where

$$\hat{H}_{e-e} = \sum_i U_d n_{i\uparrow} n_{i\downarrow} + \sum_l U_p n_{l\uparrow} n_{l\downarrow} + \sum_{\langle il\rangle} U_{pd} n_i n_l \ , \quad (9)$$

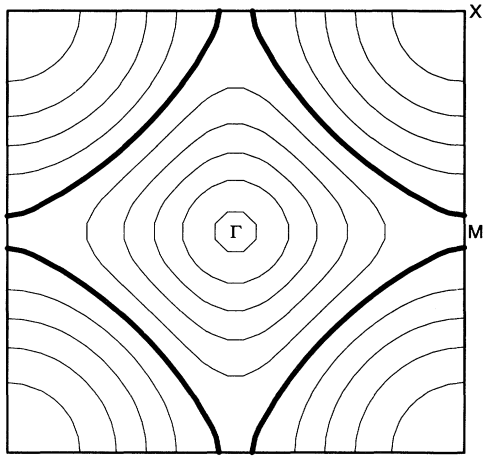

FIG. 2. The Hartree-Fock Fermi surface for a doped hole density of 0.125 (thick line). Also shown are energy band countours, in spacings of 0.5 eV relative to the Fermi energy. The Fermi surface shape and velocities fit $t = 0.66$ eV, $t' = -0.14$ eV. Two-particle Coulomb potential matrix elements fit $U = 4.0$ eV, $U' = 0.06$ eV.

and, as in Eqs. (2)–(4), index i labels the copper sites and l labels the oxygens. For brevity we have implicitly included the hole spin in the momentum label $\mathbf{k}$. This momentum space representation of the electron-electron interactions can then be mapped back to the single-band model of on-site and nearest neighbor Coulomb interactions, as in Eq. (7). The three-band values of $V(\mathbf{k}_1,\mathbf{k}_2,\mathbf{k}_3,\mathbf{k}_4)$ for a set of points on the Fermi surface are fit to the corresponding Coulomb matrix elements in a one-band model, with the effective interaction Hamiltonian in Eq. (7). We found that the best fit corresponded to values of U and U' of 4.0 eV and 0.06 eV, respectively. Notice that the Hartree-Fock values of t and U are comparable to those found by exact diagonalization, although the Hartree-Fock t is somewhat larger and the U/t ratio slightly smaller. Since U' is very small we shall neglect it in the remainder of this paper.

A. Oxygen breathing mode coupling

The oxygen breathing modes correspond to stretching of the planar copper oxygen bonds, such as the mode illustrated in Fig. 3. Clearly these modes will have a relatively large electron-phonon coupling since they directly modulate the copper-oxygen hopping. These modes also have relatively high frequencies, because of the stiff Cu-O bonds and the light oxygen mass. For example, in La_2CuO_4 the zone corner breathing mode with O_x and O_y moving in phase is at about[40] 640 cm^{-1}, and the out-of-phase mode (quadrupolar) is at about 400 cm^{-1}. In $YBa_2Cu_3O_7$ the analogous modes occur between 340 and 610 cm^{-1}, where the wider frequency range is because of mixing of plane- and chain-drived modes.[41] Very soon after the discovery of the cuprates, Fu and Freeman calculated the breathing mode frequency and obtained a large deformation potential

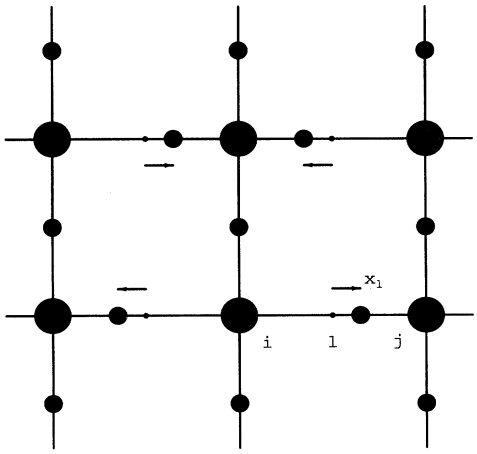

FIG. 3. A typical oxygen breathing mode. The one shown is an O_x mode at $\mathbf{Q} = (\pi, \pi)$. The true normal modes are linear combinations of such O_x and O_y modes.

of about 3 eV/Å for these modes.[19] Subsequently Weber and Mattheiss[2] found a significant overall electron-phonon interaction of $\lambda \sim 0.5 - 1$. From their plots of $\alpha^2(\omega)F(\omega)$ it is clear that the high-frequency oxygen modes contribute a substantial fraction of this overall coupling, although the lower-frequency modes are also significant.[2] More recent work again shows a significant coupling to these breathing modes, although again with again lower-frequency modes also contributing strongly. The best current LDA estimates of the overall coupling strength are $\lambda \sim 1.4$ and $\lambda \sim 1.7$ for $La_{2-x}R_xCuO_4$ and $YBa_2Cu_3O_7$, respectively.[40,41]

We have calculated the breathing mode electron-phonon coupling in the effective one-band Hamiltonian. Since this approach explicitly incorporates the electron-electron interactions, it provides an interesting counterpart to the LDA results.[2,19,40,41] In order to derive the Hamiltonian we need to consider only the simplest breathing mode oxygen displacements, such as the mode shown in Fig. 3 in which the O_x atoms move and the O_y atoms are stationary. It is clear that within an effective one-band Hamiltonian the perturbation due to O_x motion must have the following form:

$$\hat{H}^x_{e-p} = V_x \sum_{l,\sigma} (c^\dagger_{i,\sigma} c_{i,\sigma} - c^\dagger_{j,\sigma} c_{j,\sigma}) x_l, \tag{10}$$

where the sum over l includes all O_x oxygen atoms, and x_l is the displacement. Here copper sites i and j represent the two copper sites bonded to oxygen atom l. Obviously there is a similar perturbation Hamiltonian for motions of the O_y atoms. This form for the effective Hamiltonian is the only possible one which is linear in x_l, is odd under the reflection $x \to -x$, and is spatially local. It is local because a displacement of a single oxygen atom l only affects the two neighboring copper sites i and j. Locality is a good assumption in the cuprates because the one-band Wannier orbitals are well localized around each copper site. A previous report of our work[42] used an incorrect form for $\hat{H}^x_{e-p}$.

The breathing mode electron-phonon interaction Hamiltonian (10) has a single coupling parameter V_x. This can be determined uniquely by exact Lanczos diagonalization of clusters. In the Cu_4O_8 three-band model cluster we calculate the perturbation of the eigenvalues in Fig. 1 due to a small displacement of the O_x oxygens as shown in Fig. 3. We used a phonon wave vector of $\mathbf{Q} = (\pi, \pi)$ since the linear electron-phonon coupling vanishes by symmetry at $\mathbf{Q} = (0, 0)$. (We shall use the lattice constant of the CuO_2 plane, a, as the unit of length throughout this paper, where $a = 7.212a_0$ in tetragonal La_2CuO_4.) The change in the three-band ground state energy in as a function of oxygen displacement is consistent with the corresponding one-band model ground state energy only if $V_x = 8.5$ eV/a.

As a check, we also calculated the breathing mode electron-phonon coupling parameter V_x using the Hartree-Fock method. Making a frozen phonon lattice distortion as in Fig. 3 we computed the change in the self-consistent Hartree-Fock Hamiltonian $\Delta H_{\rm HF}$. We then detemined the matrix elements of this perturbation among the single particle electron states $|\langle \mathbf{k} + \mathbf{Q}|\Delta H_{\rm HF}|\mathbf{k}\rangle|^2$. Here $|\mathbf{k}\rangle$ is a state on the Fermi surface of Fig. 2. Again we used $\mathbf{Q} = (\pi, \pi)$. Comparing the full three-band matrix elements with the single-band matrix elements of Hamiltonian (10), we find $V_x = 8.3$ eV/a. The matrix elements are very insensitive to the specific electron wave vector on the Fermi surface, $\mathbf{k}$, consistent with the extreme locality assumed in Eq. (10). It is encouraging that again there is a good correspondence between the single-band electron-phonon coupling parameters derived by exact diagonalization and those obtained from the Hartree-Fock method.

III. OXYGEN TILTING MODE COUPLING

The modes with the highest phonon frequencies do not necessarily make the largest contributions to pairing, since the BCS electron-phonon coupling parameter λ decreases like $1/\omega^2$. In the cuprates the low-frequency modes arise either from motions of the heavy ions, such as Cu, La, Y, Ba, or from motions of the oxygen atoms perpendicular to the Cu-O bonds. The latter bond-bending modes include the soft modes which lead to the tilting instability of tetragonal La_2CuO_4 into its low-temperature orthorhombic phase. *Ab initio* calculations show a classic double-well potential for this tilting mode in La_2CuO_4.[20] Jahn-Teller-driven oxygen double-well potentials have also been predicted to occur in $YBa_2Cu_3O_7$ due to similar bond-bending oxygen modes.[22] Phonon anharmonicity can potentially increase the superconducting T_c well beyond the limits of conventional Eliashberg theory.[24] Jahn-Teller effects and anharmonicity have also been the basis of several theories of high-T_c superconductivity.[25,26,23] Experimentally there is some evidence for moderate anharmonicity in $YBa_2Cu_3O_7$;[27,28] however, whether the anharmonicity is strong enough to significantly enhance T_c remains unclear at this point.[29]

We have concentrated on the oxygen modes which

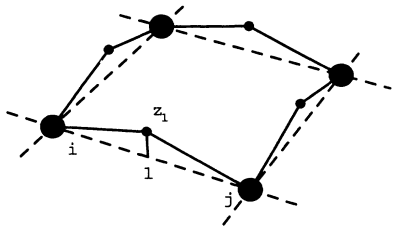

FIG. 4. A CuO_2 plane buckling mode, at $\mathbf{Q} = (0,0)$. Related modes correspond to tilting instabilities of the CuO_4 octahedra in La_2CuO_4 and have a double-well potential.

tilt or buckle the CuO_2 plane, as illustrated in Fig. 4. The mode shown is a $\mathbf{Q} = (0,0)$ mode corresponding to the static buckling (or puckering) of the plane in $YBa_2Cu_3O_7$. A related $\mathbf{Q} = (\pi,\pi)$ mode corresponds to the tilting of the CuO_4 octahedra in La_2CuO_4 in the orthorhombic phase. The procedure to determine the effective one-band electron-phonon coupling parameters for the tilting modes is similar to the breathing mode calculation. First, we displace the oxygen atoms in the z direction, relative to a perfectly flat CuO_2 sheet (defining $z = 0$). For such a displacement symmetry and locality require that the effective single-band Hamiltonian have the form[42]

$$\hat{H}^z_{e-p} = V_z \sum_{l,\sigma} (c^\dagger_{i\sigma} c_{i\sigma} + c^\dagger_{j\sigma} c_{j\sigma}) z_l^2 + V'_z \sum_{l,\sigma} (c^\dagger_{i\sigma} c_{j\sigma} + c^\dagger_{j\sigma} c_{i\sigma}) z_l^2, \tag{11}$$

where again copper sites i and j are the two neighbors of oxygen site l. This effective Hamiltonian has two types of terms, corresponding to on-site energy changes at i and j (V_z) and modulation of the effective single-band hopping (V'_z). By symmetry, the Hamiltonian is quadratic in the oxygen displacements, z_l.

To determine the parameters in Eq. (11) by exact diagonalization we calculated the perturbations in the many-body eigenvalues in Fig. 1 under the displacement shown in Fig. 4. For convenience we took a $\mathbf{Q} = (0,0)$ displacement and displaced both $x-$ and $y-$ bonded oxygen atoms, thus retaining the full lattice symmetry. Because of the quadratic dependence on z_l phonon displacements at $\mathbf{Q} = (0,0)$, $\mathbf{Q} = (\pi,0)$, or $\mathbf{Q} = (\pi,\pi)$ correspond to exactly equivalent perturbations in this model. Fitting the perturbations on the exact three-band eigenvalues with the corresponding single-band interaction Hamiltonian (11) leads to $V_z = 4.7\ \mathrm{eV}/a^2$ and $V'_z = -13.3\ \mathrm{eV}/a^2$.

We also calculated V_z and V'_z using the Hartree-Fock method. As for the x displacements, we obtained the change in the self-consistent Hartree-Fock Hamiltonian, $\Delta\hat{H}_{\mathrm{HF}}$, as a function of z_l. The matrix elements $\langle \mathbf{k}+\mathbf{Q}|\Delta\hat{H}_{\mathrm{HF}}|\mathbf{k}\rangle|^2$ as a function $\mathbf{k}$ fit very well to a perturbation of the form (11), with parameters $V_z = 8.2\ \mathrm{eV}/a^2$, $V'_z = -5.6\ \mathrm{eV}/a^2$. The slight differences from an earlier report of these results[42] are due to more accurately converged Hartree-Fock calculations in the current work. The exact diagonalization and Hartree-Fock values of the parameters are in reasonable agreement, given that the values of V_z and V'_z tend to be strongly anticorrelated in the fits to the many-body spectrum or single-particle $\mathbf{k}$ dependence.

IV. SUPERCONDUCTING TRANSITION: BREATHING MODES

The effective electron-phonon coupling Hamiltonian derived above provides a simple, parameter-free, model in which many different possible mechanisms of cuprate superconductivity can be explored. Clearly the electron-electron interactions are in the regime intermediate between weak and strong correlations ($U/t \sim 6-7$). In order to get an estimate of the strength and importance of the electron-phonon interactions we have estimated the effective coupling and T_c using the Eliashberg gap equation. The linearized gap equation defining T_c is[43]

$$\Delta(\mathbf{k},\xi) = \beta^{-1} \sum_{\mathbf{k}',\xi'} G(\mathbf{k}',\xi') G(-\mathbf{k}',-\xi') \times \left(\sum_\nu |g_{\mathbf{k},\mathbf{k}',\nu}| D_\nu(\mathbf{Q},\Omega) - V(\mathbf{Q}) \right) \Delta(\mathbf{k}',\xi'_l). \tag{12}$$

Here $G(\mathbf{k},\xi)$ is the normal state electron propagator at Matsubara frequency $\xi = (2n+1)\pi/\beta$, $\beta = 1/k_B T$, and $D_\nu(\mathbf{Q},\Omega)$ is the phonon propagator for phonon branch ν with wave vector $\mathbf{Q} = \mathbf{k} - \mathbf{k}'$ and Matsubara frequency $\Omega = \xi - \xi'$. $g_{\mathbf{k},\mathbf{k}',\nu}$ is the momentum space electron-phonon coupling, and $V(\mathbf{Q})$ is the electron-electron repulsion. This linearized gap equation has the form of an eigenvalue problem and T_c is the temperature at which the largest eigenvalue becomes unity, allowing a solution with nontrivial $\Delta(\mathbf{k},\xi)$. If some excitations other than phonons, such as antiferromagnetic spin fluctuations, are also relevant and can be described in an Eliashberg formalism, then these will add new terms to the eigenvalue equation (12), possibly increasing T_c.

Since the Fermi surface is highly anisotropic (Fig. 2), it is important to take full account of the wave vector dependence of the gap function $\Delta(\mathbf{k},\xi)$ around the Fermi surface. Furthermore, both anisotropic s-wave and d-wave solutions of the gap equation are possible. Making the usual assumption that the gap function is essentially independent of wave vector normal to the Fermi surface within a shell of order the phonon frequency around the Fermi energy, the angular dependent part of gap equation becomes

$$\lambda\Delta(k_\parallel) = \frac{2}{(2\pi)^2 \omega_E} \int \frac{dk'_\parallel}{v_F} \left(\sum_\nu |g_{\mathbf{k},\mathbf{k}',\nu}|^2 \right) \Delta(k'_\parallel). \tag{13}$$

Here ω_E is the phonon frequency, which we have assumed is an Einstein oscillator frequency independent of phonon wave vector. The angular dependence of the energy gap is determined by the eigenvector of this equation with the largest eigenvalue λ. The parameter λ defined in this way corresponds to the usual dimensionless coupling constant in BCS theory. Note that the Coulomb repulsion $V(\mathbf{Q})$

plays no role in determining the angular dependence of the gap, since $V(\mathbf{Q}) = U$ and is wave vector independent when the Coulomb repulsion is an on-site Hubbard interaction.

For the oxygen breathing modes, described by the electron-phonon Hamiltonian (10) the $\mathbf{k}$-space electron-phonon coupling parameters become

$$\sum_{\nu} |g_{\mathbf{k},\mathbf{k}',\nu}|^2 = \frac{(V_x)^2}{2M\omega_E}\{4\sin^2[(k_x - k'_x)/2] + 4\sin^2[(k_y - k'_y)/2]\}\,, \tag{14}$$

where M is the oxygen mass. Since the oxygen breathing modes are distributed from (Ref. 44) 400 to 640 cm^{-1} in La_2CuO_4, an average phonon frequency will be around 500 cm^{-1}, assuming a uniform density of states and weighting the average by $1/\omega^2$. Solving the eigenvalue problem Eq. (13) numerically leads to $\lambda = 0.57$ for s-wave pairing (A_{1g} symmetry). The computed gap $\Delta(k_{\|})$ has a very weak anisotropy, as shown in Fig. 5.

The angular gap equation also has eigenvectors with d-wave symmetry. For a $d_{x^2-y^2}$ gap (B_{2g} symmetry) we find an eigenvalue corresponding to $\lambda = 0.36$ for $\omega_E = 500$ cm^{-1}. This relatively large value of the d-wave λ arises because the pairing interaction, Eq. (14), is peaked at wave vectors $\mathbf{Q} = \mathbf{k} - \mathbf{k}' = (\pi, \pi)$ and vanishes at $\mathbf{Q} = (0, 0)$. The density of states is also highest at points on the Fermi surface near the Van Hove singularity at M, which are separated by wave vectors of around (π, π). Figure 5 shows the magnitude of the energy gap $|\Delta(k_{\|})|$ for both s and d-wave solutions.

In order to calculate T_c we solved the frequency-dependent gap equation

$$\Delta_s(\xi) = \pi\beta^{-1}\sum_{\xi'}\frac{1}{|\xi'|}f_c(\xi')\left(\lambda\frac{\omega_E^2}{\omega_E^2 + (\xi - \xi')^2} - \mu\right) \times \Delta_s(\xi'), \tag{15}$$

where $\mu = N(0)U$ and $\Delta_s(\xi)$ is the frequency-dependent gap function for s-wave pairing. In Eq. (15) $f_c(\xi')$ is a function which provides a cutoff when $|\xi'| \sim W_b$, with W_b the electronic half bandwidth. Such a cutoff function is necessary whenever $\mu \neq 0$. We used the function $f_c(\xi') = 1/\sqrt{1 + (\xi'/W_b)^2}$, since it has the correct low- and high-frequency limits, and we took $W_b = 4t$.

Using Eq. (15) we evaluated T_c for s-wave pairing with $\lambda = 0.57$ and $\omega_E = 500$ cm^{-1}. Taking $\mu = 0$, the critical temperature is $T_c = 102$ K, not far from the weak coupling BCS value of 140 K for this λ and ω_E. However, T_c drops rapidly as a function of the Coulomb repulsion $\mu = N(0)U$, as shown in Fig. 6. The physical value of $N(0)U$ is large, and of order 1.8 for the Fermi surface in Fig. 2. Such a large value of μ suppresses s-wave superconductivity to a T_c of around 10 K.

The calculated T_c for d-wave pairing is much larger. For any unconventional pairing state the frequency-dependent gap equation becomes

$$\Delta_d(\xi) = \pi\beta^{-1}\sum_{\xi'}\frac{1}{|\xi'|}f_c(\xi')\left(\lambda\frac{\omega_E^2}{\omega_E^2 + (\xi - \xi')^2}\right)\Delta_d(\xi'). \tag{16}$$

Notice that, unlike Eq. (15), there is no Coulomb pseudopotential term $\mu = N(0)U$. This is simply because for any unconventional gap function $\int dk'_{\|} U\Delta(\mathbf{k}', \xi') = 0$ and the Coulomb repulsion drops entirely out of Eq. (12). This has the simple physical interpretation that Cooper pairs with nonzero angular momentum have vanishing probability of occupying the same site at the same time, and hence they do not pay any penalty due to the strong on-site repulsion. Solving Eq. (16) numerically gives $T_c = 33$ K for doped La_2CuO_4. This is relatively close to the weak coupling BCS T_c of 49 K for this λ and ω_E. Since the d-wave T_c is independent of $N(0)U$, it is clear that d-wave superconductivity is favored over s-wave superconductivity when $N(0)U$ is large. Figure 6 shows that d-wave pairing will occur whenever $N(0)U > 0.4$. The calculated d-wave T_c of 33 K is close to the experimental value for doped La_2CuO_4, implying that only a small additional contribution from antiferromagnetic spin fluctuations may be needed to explain the superconductivity. Of course, it remains to be clearly established experimentally that doped La_2CuO_4 is a d-wave superconductor, since most of the relevant experiments have so far only been carried out on $YBa_2Cu_3O_7$.

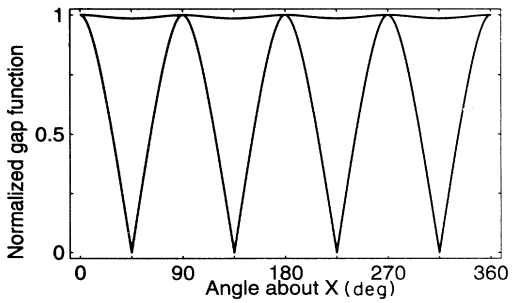

FIG. 5. Angular dependence of the gap function, $|\Delta(k_{\|})|$, for s- and d-wave solutions, plotted as a function of angle around the Fermi surface. The angles are measured about the X point in the zone.

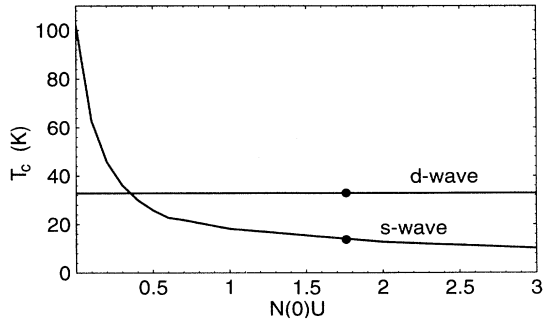

FIG. 6. Calculated T_c for doped La_2CuO_4 as a function of electron-electron repulsion parameter, $\mu = N(0)U$. At the physical value of μ of 1.8 the $d_{x^2-y^2}$ $T_c \approx 30$ K, while the s-wave T_c is suppressed to ≈ 10 K.

The above T_c calculations strictly apply only to doped La_2CuO_4, since the original many-body Hamiltonian parameters[15] were determined for this system. Any estimates of T_c in other materials, such as $YBa_2Cu_3O_7$ must necessarily have somewhat greater uncertainty. If we assume the same many-body Hamiltonian parameters and Fermi surface, then the only difference is in the phonon frequencies. For $YBa_2Cu_3O_7$ the oxygen breathing mode frequencies are in the range[41] 340–610 cm^{-1}, leading to an estimated average frequency of about 450 cm^{-1}. This implies $\lambda = 0.70$ for s-wave pairing and 0.44 for d-wave superconductivity, slightly higher than the La_2CuO_4 values. These estimates lead to $T_c = 52$ K in the $d_{x^2-y^2}$ channel, with again s-wave superconductivity strongly suppressed by the large Coulomb repulsion. The difference from the experimental T_c of 92 K could be due to contributions from antiferromagnetic spin fluctuations,[8] differences in the effective Hamiltonian or coupling between $YBa_2Cu_3O_7$ and La_2CuO_4, or due to possible enhancements in T_c resulting from the double layer structure of the unit cell.[45]

V. SUPERCONDUCTING TRANSITION: TILTING MODES

As well as the high-frequency oxygen breathing modes our Hamiltonian also includes coupling to the out-of-plane modes which tilt or buckle the CuO_2 plane. These modes have a double-well structure

$$V_{\rm ion}(z) = -\alpha z^2 + \beta z^4 \tag{17}$$

in La_2CuO_4-derived compounds.[20] A standard Eliashberg formalism does not apply to phonons with double-well energies such as these. Calculations of superconductivity due to these modes would go beyond the scope of this paper. Nevertheless, we can make two simple estimates of the importance of these modes using an Eliashberg approach.

First we can approximate the double-well potential by a harmonic well centered at one of the minimia, $z_0 = \sqrt{\alpha/2\beta}$, and with frequency corresponding to $M\omega_E^2 = 2\alpha$. This is appropriate for the limit of a large barrier height in $V_{\rm ion}(z)$. The calculated barrier height is around 25 meV, compared to a measured frequency of $\omega_E = 100$ $cm^{-1} = 12$ meV.[44] The experimental tilting angle of 5° gives $z_o = 0.044a$. Expanding the electron-phonon Hamiltonian Eq.(11) to linear order in $z - z_0$ gives

$$\sum_\nu |g_{\mathbf{k},\mathbf{k}',\nu}|^2 = \frac{(2z_0)^2}{2M\omega_E}\{|2V_z\cos[(k_x-k_x')/2] + 2V_z'\cos[(k_x+k_x')/2]|^2 + |2V_z\cos[(k_y-k_y')/2] + 2V_z' \times \cos[(k_y+k_y')/2]|^2\}. \tag{18}$$

Solving the angular dependent gap equation (13) with this coupling leads to $\lambda = 0.14$ for s-wave pairing and $\lambda = 0.095$ for $d_{x^2-y^2}$ superconductivity. Such small values of λ could contribute slightly to the superconductivity, but could not lead to high-T_c superconductivity alone.

Alternatively, we can estimate the effect of tilting modes on the superconductivity due to the *quadratic* part of the coupling. Quadratic coupling leads to a process where *two* phonons are exchanged. The relevant gap equation becomes

$$\Delta(\mathbf{k},\xi) = \beta^{-2}\sum_{\mathbf{k}',\xi',\mathbf{q},\omega} G(\mathbf{k}',\xi')G(-\mathbf{k}',-\xi') \times \left(\sum_\nu |g_{\mathbf{k},\mathbf{k}',\nu}|^2\right) D_\nu(\mathbf{Q}-\mathbf{q},\Omega-\omega)D_\nu(\mathbf{q},\omega) \times \Delta(\mathbf{k}',\xi_l'), \tag{19}$$

omitting the Coulomb repulsion term. Here $\mathbf{q}$ and $\omega = 2n\pi/\beta$ are the wave vector and Matsubara frequency of the second phonon, and otherwise the notation is the same as Eq. (12). The quadratic electron-phonon coupling is

$$\sum_\nu |g_{\mathbf{k},\mathbf{k}',\nu}|^2 = \frac{1}{(2M\omega_E)^2}\{|2V_z\cos[(k_x-k_x')/2] + 2V_z'\cos[(k_x+k_x')/2]|^2 + |2V_z\cos((k_y-k_y')/2) + 2V_z'\cos((k_y+k_y')/2)|^2\}. \tag{20}$$

Defining the dimensionless coupling parameter λ as the largest eigenvalue of the angular-dependent gap equation (13) we obtain $\lambda = 0.013$ for s-wave pairing and $\lambda = 0.009$ for d-wave superconductivity. These values of λ are too small to make any significant contribution to T_c.[46]

VI. CONCLUSION

In summary, we have derived an effective single-band Hamiltonian for the cuprates which includes both electron-electron repulsion and electron-phonon coupling. The Hamiltonian was derived directly from the *ab-initio* DFT multiple-band Hubbard Hamiltonian of McMahan *et al.*[15] As such it combines a realistic, parameter-free, model of the electronic structure and electron-electron interactions. The electron-phonon coupling matrix elements are derived in a way which explicitly takes into account the strong electron-electron interactions, unlike, say, electron-phonon coupling calculations based upon Kohn-Sham band structures. The Hamiltonian is specifically designed to incorporate the low-energy physics of copper oxide planes as accurately as possible, including the realistic Fermi surface shape, Fermi surface band velocities, and the electron-electron and electron-phonon interactions experienced by electrons and holes at the Fermi surface. We include both the coupling to in-plane oxygen breathing modes and to the anharmonic out of plane tilting modes. Our full many-body single-band Hamiltonian is the following:

$$\hat{H} = \hat{H}_e + \hat{H}_{e-e} + \hat{H}^x_{e-p} + \hat{H}^z_{\rm el-p}\ , \tag{21}$$

where

$$\hat{H}_e = t \sum_{\langle i,j\rangle,\sigma} (c^\dagger_{i,\sigma} c_{j,\sigma} + \text{H.c.}) + t' \sum_{\langle\langle i,k\rangle\rangle,\sigma} (c^\dagger_{i,\sigma} c_{k,\sigma} + \text{H.c.}) , \tag{22}$$

$$\hat{H}_{e-e} = U \sum_i n_{i\uparrow} n_{i\downarrow} + U' \sum_{\langle i,j\rangle} n_i n_j , \tag{23}$$

$$\hat{H}^x_{e-p} = V_x \sum_{l,\sigma} (c^\dagger_{i,\sigma} c_{i,\sigma} - c^\dagger_{j,\sigma} c_{j,\sigma}) x_l , \tag{24}$$

$$\hat{H}^z_{\text{el}-p} = V_z \sum_{l,\sigma} (c^\dagger_{i,\sigma} c_{i,\sigma} + c^\dagger_{j,\sigma} c_{j,\sigma}) z_l^2 , \\ + V'_z \sum_{\langle i,j\rangle,\sigma} (c^\dagger_{i,\sigma} c_{j,\sigma} + c^\dagger_{j,\sigma} c_{i,\sigma}) z_l^2 . \tag{25}$$

The specific parameter values are summarized in Table I. These values are appropriate for La_2CuO_4-based compounds, but would presumably be similar in all other materials with CuO_2 planes.

We have shown that a standard Eliashberg formalism applied to this Hamiltonian predicts high-T_c superconductivity in a $d_{x^2-y^2}$ channel. The predicted T_c values are 33 K for doped La_2CuO_4 and an estimated 52 K for $YBa_2Cu_3O_7$. d-wave superconductivity is favored because of the strong Coulomb repulsion U, which strongly reduces the s-wave T_c, as illustrated in Fig. 6. The Eliashberg equations we have used do not include higher-order electron correlation effects, such as the exchange of antiferromagnetic spin fluctuations, which may further increase the d-wave T_c above the values reported here. Nor do our calculations include strong coupling effects beyond Eliashberg theory, such as vertex corrections[47] or polaron formation.[48] It is not clear whether these effects are important given the intermediate size of the dimensionless electron-phonon coupling parameter, $\lambda \sim 0.35-0.7$, derived here. Certainly our predicted electron-phonon coupling parameters are not as large as some estimates based upon the extreme strong coupling limit of s-wave superconductivity.[49] On the other hand, our calculated values of λ are reasonably consistent with LDA calculations,[40,41] given that we only include a subset of the full spectrum of phonon modes.

Recent photoemission measurements[50] of the temperature-dependent gap anisotropy $Bi_2Sr_2Ca_1Cu_2O_{8+x}$ also have a natural explanation in terms of Fig. 6. The gap was measured along the $\Gamma - X$ direction (in the notation of Fig. 2). At and just below T_c the gap was unobservably small in this direction while being quite large on other parts of the Fermi surface. This is as expected in a pure $d_{x^2-y^2}$ superconductor. Further below T_c the gap along $\Gamma - X$ became nonzero, indicating a change of order parameter symmetry. A symmetry analysis and Ginzburg-Landau calculation indicates that the data are consistent with a two-order-parameter picture in which s and $d_{x^2-y^2}$ order parameters become mixed due to the slight orthorhombic lattice distortion.[51] The pure d-wave T_c is higher than the pure s-wave T_c, implying strong temperature dependence to the order parameter mixing between the two transition temperatures, as observed experimentally. This two-order-parameter picture is qualitatively consistent with our results shown in Fig. 6.

TABLE I. The effective single-band Hamiltonian parameter values derived by exact diagonalization of clusters (Lanczos) or by the Hartree-Fock (HF) method. All energies are given in eV, and distances are measured in units of the CuO_2 plane lattice spacing a.

	Lanczos	HF
t	0.48	0.66
t'		-0.14
U	3.2	4.0
U'		0.06
V_x	8.5	8.3
V_z	4.7	8.2
V'_z	-13.3	-5.6

Whatever the complete explanation of high-temperature superconductivity, the electron-phonon Hamiltonian derived above should provide a useful starting point for calculations of both normal and superconducting state properties of high-T_c superconductors. At the very least it should provide a realistic starting point for studies investigating the competing effects of phonon-mediated attraction and strong on-site Hubbard repulsion in the cuprates.[52,53] Phonon anharmonicity can easily be incorporated into our Hamiltonian, which may also provide mechanisms for enhancements in the superconducting transition temperatures.[25,26]

ACKNOWLEDGMENTS

This work was supported by the Office of Naval Research. We thank Joao Florencio, Jr. for useful discussions, and we thank R. Joynt, M. Onellion, and C. Quitmann for communicating their unpublished results to us.

* Present address: Department of Physics, Technion-Israel Institute of Technology, Haifa 32000 Israel.
† Present address: University of Bristol, H.H. Wills Physics Laboratory, Royal Fort Tyndal Avenue, Bristol BS8 1TL, UK.

[1] J.G. Bednorz and K.A. Müller, Z. Phys. B **64**, 188 (1986); C.W. Chu *et al.*, Phys. Rev. Lett. **58**, 405 (1987).
[2] W. Weber, Phys. Rev. Lett. **58**, 1371 (1987); W. Weber and L.F. Mattheiss, Phys. Rev. B **37**, 599 (1988).
[3] B. Batlogg *et al.*, Phys. Rev. Lett. **58**, 2333 (1987); L.C. Bourne *et al.*, *ibid.* **58**, 2337 (1987); K.J. Leary *et al.*, *ibid.* **59**, 1236 (1987); D.E. Morris *et al.*, *ibid.* **37**, 5936 (1988).
[4] N. Bulut and D.J. Scalapino, Phys. Rev. B **45**, 2371 (1992); J.A. Martindale *et al.*, Phys Rev. B **47**, 9155 (1993).

[5] X.K. Chen, J.C. Irwin, R. Liang, and W.N. Hardy, Physica C **277** 113 (1994).
[6] J.F. Annett, N. Goldenfeld, and S.R. Renn, Phys. Rev. B **43**, 2778 (1991); W.N. Hardy *et al.*, Phys. Rev. Lett. **70**, 3999 (1993); J.E. Sonier *et al.*, *ibid.* **72**, 744 (1994).
[7] D.A. Wollman *et al.*, Phys. Rev. Lett. **71**, 2134 (1993).
[8] K. Mikaye, S. Shmitt-Rink, and C.M. Varma, Phys. Rev. B **34**, 6554 (1988); D.J. Scalapino, E. Loh, Jr., and J.E. Hirsch, *ibid.* **34**, 8190 (1988); H. Chu and E.W. Fenton, *ibid.* **42**, 6408 (1990); P. Monthoux and D. Pines, Phys. Rev. Lett. **69**, 961 (1992).
[9] C. Gros, R. Joynt, and T.M. Rice, Z. Phys. B **68**, 425 (1987); S.R. White *et al.*, Phys. Rev. B. **39**, 839 (1989); E. Dagotto *et al.*, *ibid.* **49**, 3548 (1994).
[10] M.C. Krantz, C. Tomsen, Hj. Mattausch, and M. Cardona, Phys. Rev. B **50**, 1165 (1994); A.P. Litvinchuk *et al.*, *ibid.* **50**, 1171 (1994); G. Blumberg *et al.*, J. Supercond. **7**, 445 (1994).
[11] B. Batlogg *et al.*, Phys. Rev. Lett. **61**, 1670 (1988); D.G. Hinks *et al.*, Nature **335**, 419 (1988); C.K. Loong *et al.*, Phys. Rev. Lett. **62**, 2628 (1989); S. Kondoh, M. Sera, Y. Ando, and M. Sato, Physica C **157**, 469 (1989); E.S. Hellman, *ibid.* **211**, 486 (1993).
[12] D. Ho *et al.*, Phys. Rev. Lett. **70**, 85 (1993).
[13] H. Chen and J. Callaway, Phys. Rev. B **46**, 14321 (1992).
[14] J.P. Franck *et al.*, Phys. Rev. Lett. **71**, 283 (1993).
[15] A.K. McMahan, R.M. Martin, and S. Satpathy, Phys. Rev. B **38**, 6650 (1988); A.K. McMahan, J.F. Annett, and R. M. Martin, *ibid.* **42**, 6268 (1990).
[16] M.S. Hybertsen, M. Schluter, and N.E. Christensen, Phys. Rev. B **39**, 9028 (1989).
[17] M.S. Hybertsen *et al.*, Phys. Rev. B **41**, 11068 (1990).
[18] S.B. Bacci, E.R. Gagliano, R.M. Martin, and J.F. Annett, Phys. Rev. B **44**, 7504 (1991).
[19] C.L. Fu and A.J. Freeman, Phys. Rev. B **35**, 8861 (1987).
[20] R.E. Cohen, W.E. Pickett, and H. Krakauer, Phys. Rev. Lett. **64**, 2575 (1990); W.E. Pickett, Rev. Mod. Phys. **61**, 433 (1989).
[21] R.E. Cohen, W.E. Pickett, and H. Krakauer, Phys. Rev. Lett. **62**, 831 (1989); W.E. Pickett, R.E. Cohen, and H. Krakauer, *ibid.* **67**, 228 (1991).
[22] K.H. Johnson, D.P. Clougherty, and M.E. McHenry, Mod. Phys. Lett. B **18**, 1367 (1989); in *Electronic Structure and Mechanisms for High Temperature Superconductivity*, edited by J. Ashkenazi and G. Vezzoli (Plenum, New York, 1991).
[23] R.S. Markiewicz, Physica C **200**, 65 (1992).
[24] J.R. Hardy and J.W. Flocken, Phys. Rev. Lett. **60**, 2191 (1988).
[25] A. Bussmann-Holder and A.R. Bishop, Phys. Rev. B **44**, 2853 (1991).
[26] See, for example, the articles by J.R. Hardy, J.W. Flocken, and R.A. Guenther, by N.M. Plakida, T. Galbaatar, S.L. Drechsler, and S. Krasavin, and by A. Bussmann-Holder and A.R. Bishop, in *Lattice Effects in High T_c Superconductors*, edited by Y. Bar Yam, T. Egami, J. Mustre-de Leon, and A.R. Bishop (World Scientific, Singapore, 1992).
[27] V.H. Crespi and M.L. Cohen, Solid State Commun. **86**, 161 (1993).
[28] W. Reichardt *et al.*, J. Supercond. **7**, 399 (1994); M. Arai *et al.*, *ibid.* **7**, 415 (1994).
[29] R. Heid and H. Rietschel, Phys. Rev. B **44**, 734 (1991).
[30] E.B. Stechel and D.R. Jennison, Phys. Rev. B **38**, 4632 (1988).
[31] B.H. Brandow, J. Solid State Chem. **88**, 28 (1990).
[32] J.F. Annett, R.M. Martin, A.K. McMahan, and S. Satpathy, Phys. Rev. B **40**, 2620 (1989).
[33] V.I. Anisimov, J. Zaanen, and O.K. Anderson, Phys. Rev. B **44**, 943 (1991).
[34] M.T. Czyzyk and G.A. Sawatzky, Phys. Rev. B **49**, 14211 (1994).
[35] W. A. Harrison, *Electronic Structure and the Properties of Solids* (Freeman, San Francisco, 1980).
[36] L.F. Mattheiss, Phys. Rev. Lett. **58**, 1028 (1987).
[37] J. Yu, A.J. Freeman, and J.-H. Xu, Phys. Rev. Lett. **58**, 1035 (1987).
[38] D.C. Mattis and M.P. Mattis, in *Theories of High Temperature Superconductivity*, edited by J. Woods Halley (Addison-Wesley, Redwood City, CA, 1988), p. 79.
[39] D.M. Newns, P.C. Pattnaik, and C.C. Tsuei, Phys. Rev. B **43**, 3075 (1991).
[40] H. Krakauer, W.E. Pickett and R.E. Cohen, in *Lattice Effects in High-T_c Superconductors*, Ref. 26.
[41] I.I. Mazin *et al.*, in *Lattice Effects in High-T_c Superconductors*, Ref. 26.
[42] J. Song and J.F. Annett, J. Superconduct. **7**, 925 (1994).
[43] G. Rickayzen, *Green's Functions and Condensed Matter Physics* (Academic Press, London, 1980).
[44] C. Thomsen and M. Cardona, in *Physical Properties of High Temperature Superconductors I*, edited by D.M. Ginsberg (World Scientific, Singapore, 1989).
[45] I. Morgensterm, Th. Husslein, J.M. Singer, and H.G. Matuttis, J. Phys. I (France) **3**, 1043 (1993); Y.M. Malozovsky, S.M. Bose, P. Longe, and J.D. Fan, Phys. Rev. B **48**, 10504 (1993); S. Chakravarty and P.W. Anderson, Phys. Rev. Lett. **72**, 3859 (1994).
[46] Our earlier report of our calculations, Ref. 42, contained significant errors in estimates of T_c due to the tilting modes.
[47] L. Pietronero and S. Strassler, Europhys. Lett. **18**, 627 (1992).
[48] A.S. Alexandrov, Phys. Rev. B **38**, 925 (1988); Physica C **191**, 115 (1992).
[49] R. Zeyher and G. Zwicknagel, Solid State Commun. **66**, 617 (1988); L.N. Bulaevski, O.V. Dolgov, A.A. Golubov, M.O. Pittsyn, and S.I. Vedeneev, Mod. Phys. Lett. B **3**, 101 (1989).
[50] J. Ma, C. Quitmann, R.J. Kelley, H. Berger, G. Margaritondo, and M. Onellion (unpublished).
[51] J. Betouras and R. Joynt (unpublished).
[52] H.B. Schuttler and A.J. Fedro, Phys. Rev. B **45**, 7588 (1992); H.B. Schuttler, J. Zhong and A.J. Fedro, in *Electronic Properties and Mechanisms of High T_c Superconductors*, edited by T. Oguchi, K. Kadowaki, and T. Sasaki (Elsevier, New York, 1992).
[53] A. Muramatsu and W. Hanke, Phys. Rev. B **38**, 878 (1988); R.T. Scalettar, N.E. Bickers, and D.J. Scalapino, *ibid.* **40**, 197 (1989); T. Egami, S. Ishihara, and T. Tachiki, Science **261**, 1307 (1993); J. Zielinski and M. Matlak, Phys. Lett. A **172**, 467 (1993); J.H. Kim and Z. Tesanovic, Phys. Rev. Lett. **71**, 4218 (1993).